Trees (2016) 30:1361–1375
DOI 10.1007/s00468-016-1373-x

ORIGINAL ARTICLE

Foliar phase changes are coupled with changes in storage and biochemistry of monoterpenoids in western redcedar (*Thuja plicata*)

Adam J. Foster[1,2] · Roni Aloni[3] · Mario Fidanza[1,4] · Regine Gries[1] · Gerhard Gries[1] · Jim Mattsson[1]

Received: 5 August 2015 / Accepted: 19 February 2016 / Published online: 9 March 2016

Abstract

Key message **The monoterpenoid content of *Thuja plicata* needles and scales differs both quantitatively and qualitatively. Resin storage structures are associated with anatomical modifications that suggest facilitated exit of monoterpenoids.**

Abstract Western redcedar (*Thuja plicata*) is a highly valued source of lumber. *T. plicata* trees planted in reforestations efforts are often heavily damaged by extensive ungulate browsing. Research has shown that high foliar content of monoterpenoids deters browsing, providing an avenue for resistance selection in young plants. *T. plicata* foliage undergoes, however, extensive phase changes during early growth. Currently it is unknown whether the anatomical basis of monoterpenoid storage and release, and the content and composition of stored monoterpenoids, also change at the same time. Here, we studied these aspects of *T. plicata* seedling biology. Cotyledons lack storage structures for terpenoids. Needles contain a single longitudinal terpenoid duct with (+)-sabinene and (−)-α-pinene as prevalent monoterpenoids. In contrast, scales contain enclosed resin glands and have a monoterpenoid profile that is markedly different from needles, with α-thujone as the most prevalent monoterpenoid and no detectable levels of (−)-α-pinene. Both ducts and glands are close to the epidermis and vascular tissues, frequently companioned by gaps in the sub-epidermal fiber layer, suggesting paths of facilitated diffusion of monoterpenoids out of tissues. We conclude that foliar phase changes are coupled with equally significant changes in resin storage structure anatomy, monoterpenoid levels and composition. Our findings provide a framework for reproducible sampling and selection not only for high levels of monoterpenoids but also for anatomical markers that may affect release of these compounds.

Keywords Western redcedar · *Thuja plicata* · Monoterpenes · Ontogeny · Metamorphic heteroblasty · Resin ducts · Resin glands · α-Thujone · Herbivory

Communicated by A. Gessler.

Electronic supplementary material The online version of this article (doi:10.1007/s00468-016-1373-x) contains supplementary material, which is available to authorized users.

✉ Jim Mattsson
jmattsso@sfu.ca

[1] Department of Biological Sciences, Simon Fraser University, 8888 University Drive, Burnaby, BC V5A1S6, Canada

[2] Present Address: Grain and Oil Seed Pathology, Charlottetown Research and Development Centre, Agriculture and Agri-Food Canada, 440 University Avenue, Charlottetown, PE C1A 4N6, Canada

[3] Department of Molecular Biology and Ecology of Plants, Tel Aviv University, 69978 Tel Aviv, Israel

[4] Present Address: Department of Pediatrics, Child and Family Research Institute, University of British Columbia, Vancouver, BC V5Z 4H4, Canada

Introduction

Western redcedar *(Thuja plicata* Donn ex Don*)* is native to the Pacific Northwest. In Canada it is unique to British Columbia (BC). Wood of *T. plicata* is highly valued due to its aesthetics, dimensional stability and natural durability. On average, 8 million seedlings are planted annually in BC (Gonzalez 2004). The BC forestry industry is facing particular difficulties with *T. plicata* reforestation because planted seedlings are extensively browsed by ungulates,

such as deer, elk and moose (Martin and Daufresne 1999; Martin and Baltzinger 2002; Vourc'h et al. 2002a, c; Stroh et al. 2008). Browsing by Sitka black-tailed deer (*Odocoileus hemionus sitkensis*) populations is the primary factor that prevents regeneration of *T. plicata* on the Haida Gwaii Islands (Stroh et al. 2008). There is, however, evidence that *T. plicata* has an innate defense against deer browsing, as plants with high foliar monoterpenoid content are browsed less heavily than those with low monoterpenoid content (Vourc'h et al. 2002a; Russell 2008).

Volatile monoterpenoids and sesquiterpenoids as well as non-volatile diterpenoids are key components of stored oleoresins in conifers and function in chemical defense against insects and microbes (Langenheim 1969, 1990, 1994; Unsicker et al. 2009). Monoterpenes are 10-carbon terpenes that are derived from geranyl diphosphate produced from the isoprenoid biosynthetic pathway. Geranyl diphosphate is converted into linear or cyclic monoterpenes by a group of proteins termed monoterpene synthases (Bohlmann et al. 1998). The genes encoding these enzymes have been cloned and characterized for many conifers, including (+)-sabinene synthase and hydroxylase from *T. plicata* (Foster et al. 2013; Gesell et al. 2015), and an α-pinene synthase from *Chamaecyparis formosensis* (Cupressaceae; Chu et al. 2009). The foliar terpene profile of mature *T. plicata* foliage varies little among populations across the trees' natural range, with α-thujone, β-thujone and sabinene being the three major monoterpenes, and α-thujene, α-pinene, myrcene, and 1*R*-(+)-limonene occurring at significant but lesser levels (Von Rudloff et al. 1988; Kimball et al. 2005).

Oleoresin-producing structures have been studied in some conifer species. Resin ducts of Aleppo pine (*Pinus halepensis*), e.g., reportedly originate from the apical meristem and form networks that correlate with the presence of vascular tissues (Werker and Fahn 1969). These ducts show variation in the number and overall size of epithelial cells relative to the developmental stage of the tissues (Werker and Fahn 1969). Characteristic features of resin storage ducts are highly heritable in Norway spruce (*Picea abies*), and the number of resin ducts show a strong correlation with monoterpenoid content in needles of lodgepole pine (*Pinus contorta*; White and Nilsson 1984; Rosner and Hannrup 2004). The ontogenetic age of needles is also an important factor in the number of resin canals in *Pinus sylvestris* (Lin et al. 2001).

Foliage and resin storage structures of all cypress members thus far studied have subulate or awl-shaped needle-like leaves (Suzuki 1979), with many species developing scale-like leaves as they mature. Specifically, *T. plicata* has large, central, abaxial resin glands in the scale-like leaves, often with multiple smaller glands present at the base of scales (Suzuki 1979). To our knowledge, there are no publications that describe the resin storage structures of *T. plicata* in any further detail. Here we refer to the juvenile subulate needle-like leaves as needles and to the scale-like leaves as scales. Although not described as such by Suzuki (1979), the phase change in *T. plicata* leaf morphology from needles in an early or juvenile form to radically different scales in a later or adult form exemplifies metamorphic heteroblasty (Reviewed by Zotz et al. 2011). This phenomenon is better known in dicot species such as the European ivy (*Hedera helix*) and some *Acacia* species (Goebel 1913; Kaplan 1980; Taiz and Zeiger 2010). With this in mind, an obvious question is to what extent these phase changes affect the anatomy and biochemistry of terpenoid biology in *T. plicata*. This question is important, as studies aiming at identifying genetic variation in terpenoid content could potentially be confounded by changes in terpenoid content due to the phase changes occurring in the early life of *T. plicata* when screens are most conveniently done. Working on *T. plicata*, we show anatomical changes in terpenoid storage as well as vast qualitative changes in terpenoid content that correlate with the changes in leaf morphology.

Materials and methods

Thuja plicata seedlings, derived from seedlots 45010, 45052, 63110, that had been grown for one season and frozen, were provided by Pacific Regeneration Technologies Inc. (Pitt Meadows, BC, Canada). They were planted in 3.8 L pots using standard peat–vermiculite mix, and grown in a greenhouse (16 h light) for 3 weeks before monoterpene extraction and anatomical studies. Anatomical studies were also done on wild seedlings collected at multiple locations and times on Burnaby Mountain, BC.

We refer to a leaf as a needle when >50 % of it is not attached to the shoot axis, and as a scale when <50 % of it is attached to the shoot axis. We refer to resin storage organs as ducts when they have a clearly visible section of even width, and resin storage organs as glands when they lack a visible portion of even width and appear spindle shaped.

Five or more seedlings were used to support each anatomical observation. Various techniques were used to visualize morphological and anatomical features. Foliage was visualized in a flatbed scanner (Figs. 1a, 2a, 9a). Leaves and sections were mounted in 30 % glycerol and photographed with a Canon Rebel EOS5 MarkI camera fitted with a Canon MP-E 65-mm macro lens or with a Nikon Eclipse E600 microscope. To facilitate light penetration, either the abaxial surface (Fig. 2b) or the adaxial surface (Figs. 4b, 5, 6a–f) was removed with a fine syringe

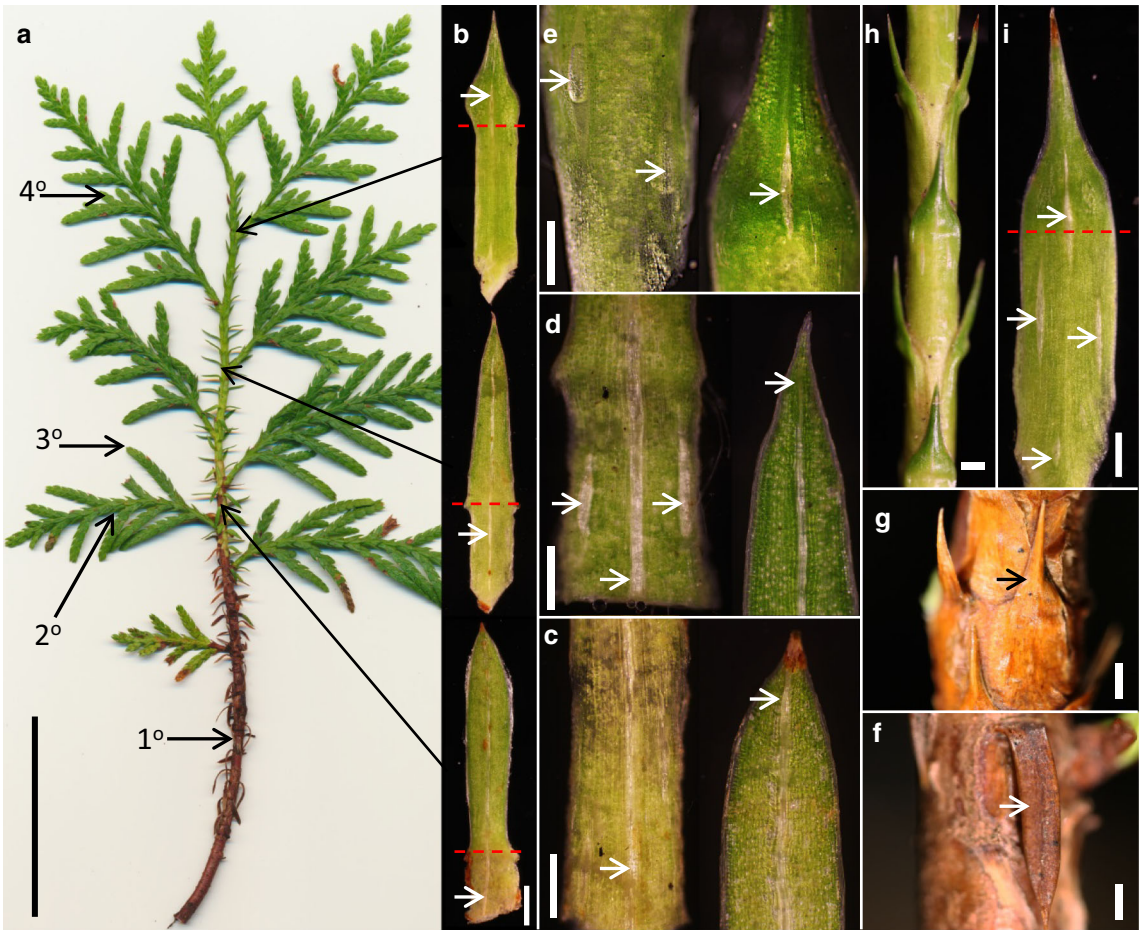

Fig. 1 Morphology of the primary shoot of a *T. plicata* seedling. **a** A 25-cm tall wild-grown seedling, with primary shoot (1°) and lateral secondary (2°) shoots. **b** Needles taken off the seedling in (**a**) from positions indicated by *arrows*, with one portion of needle (below *dashed red line*) fused to the stem, the other (above *dashed red line*) being the free blade. **c**–**e** Basal (*left*) and apical portions (*right*) of individual needles. **c** A needle with an extended section of blade margins having a central duct running from the base of the stem portion (*arrow* in the *left portion* of *picture*) to the tip of the blade (*arrow* in the *right portion* of the *picture*), with or without short lateral glands at the base (not shown). **d** A needle with a blade that is tapering in width, and has a central duct running from the base to the tip (*arrows*), and also lateral glands in the stem portion (*arrows*). **e** A needle close to the apex of the primary shoot lacking a long central duct, and instead having a central gland in the short scale-type blade, and lateral glands in the stem portion (*arrows*). **f**–**i** Primary shoot needles from a 40-cm tall wild-grown seedling. **f** Basal needles and stem surface have turned brown, **g** older scales are also browning, and **h** apical scales have an extensive portion attached to the stem relative to the free blade, **i** with several spindle-shaped glands (*arrows*). *Size bars* 50 mm in **a**; 1 mm in **b**, **f**–**i**; 0.5 mm in **c**–**e**

needle. Partial clearing and autostaining of duct and gland epithelium were obtained by vacuum infiltration in 30 % glycerol followed by mounting under coverslips and incubation at room temperature for 1–2 days before photographs were taken (Figs. 3, 6, Suppl. Figure 2). Chlorophyll was removed by overnight immersion in a solution of ethanol and glacial acetic acid (6:1), and by consecutive washes in 100 and 70 % ethanol, followed by lactic acid clearing at 95 °C for 1 h (Figs. 4a, 6, 8, Suppl. Figure 3). Sections of fresh leaves with an estimated thickness of 50–100 µm (Fig. 4) and 20–30 µm (Fig. 7) were generated by hand under a stereomicroscope, using thin razor blades lubricated by water. Sections were degassed in water by vacuum application, mounted in 30 % glycerol and then immediately photographed. Photographs of sections were taken under fiberoptic epi-illumination (Figs. 1b–f, 2b–d, 3a–d), dark-field (Fig. 5f), a combination of epi-illumination and transmitted light (Fig. 3b), transmitted Differential Interference Contrast (Figs. 4a, d–h, 5a–e, 6, 7), UV epi-fluorescence and blue light emission filtering (Nikon UV-2E/C fluorescence filter combination with 340–380 nm bandpass, 400 nm longpass, 435–485 nm bandpass, Fig. 8;

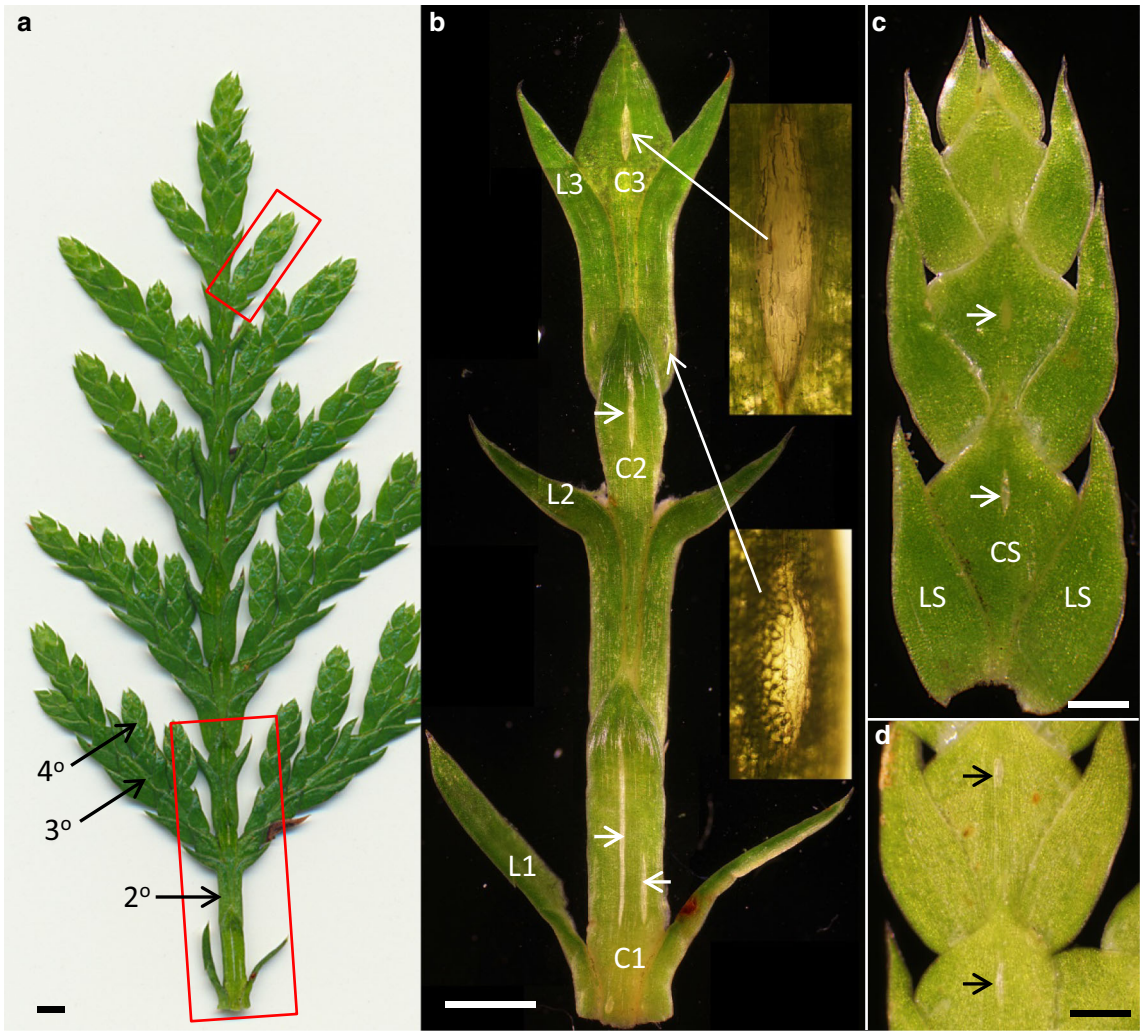

Fig. 2 Morphology of a secondary shoot. **a** A secondary (2°) shoot taken from the *T. plicata* seedling in Fig. 1, with indicated tertiary (3°) and quaternary (4°) shoots. **b** Enlargement of framed basal part in (**a**) with tertiary shoots and the backside removed, observing changes in length and shape of the central leaves (*C1*, *C2*, *C3*), and lateral leaves (*L1*, *L2*, *L3*), transitioning from needle to scale-type leaves. In addition, the central resin duct (*arrows*) becomes gradually shorter. Higher-magnification insets indicate that resin glands are close to the surface. **c** Adaxial side of young tertiary shoot framed near the *top* in (**a**), showing the typical shape of later scales (*LS*) and central scale (*CS*). Central glands are indicated with *arrows*. **d** Abaxial side of the tertiary shoot in (**c**) has a paler color, and is flatter than the adaxial side. *Arrows* point at central glands. *Size bars* 1 mm in **a**, **b**; 0.5 mm in **c**, **d**

Biggs 1985). Images were compiled in Adobe Photoshop CS5, and the contrast observed in the microscope was restored in images by limited use of the smart sharpen function.

Monoterpenes from leaves were extracted from five plants for seed batches 45010 and 45052, and from four plants for seed batch 63110, following a procedure modified from Kimball et al. (2005). For each plant, 250 mg of tissue was frozen in liquid nitrogen and ground to a fine powder using a mortar and pestle. Tissue was transferred to a 10-mL glass tube and extracted with 2 (needles) and 5 (scales) mL of ethyl acetate on a horizontal shaker for 30 min. To remove solid tissue, extracts were passed through a glass wool filter. Extracts were then concentrated under a nitrogen stream, and aliquots were analyzed by coupled gas chromatography–mass spectrometry (GC–MS) as described by Foster et al. (2013). Differences in monoterpene content between different clone lines and tissue types were determined by ANOVA followed by least squares means test using Tukeys' HSD (honest significant difference) with JMP 9 (SAS Institute).

Results

All wild-grown and purchased *T. plicata* seedlings we examined followed the same pattern of changes in leaf morphology and resin gland anatomy. Here we will

summarize morphological changes, followed by analyses of the parallel changes in the anatomy of resin storage structures and the monoterpenoid content of needles and scales.

Phase changes of leaf and resin organ morphologies in *T. plicata* seedlings

The primary shoot

The cotyledons lack any visible resin storage organ (not shown). A 20 to 25-cm tall wild seedling (Fig. 1a) has a primary shoot (1°) with a number of secondary shoots (2°). Leaves along the primary shoot gradually transit from needles to scales (Fig. 1b). In the same order, resin duct organization changes from a central abaxial duct along the complete needle (Fig. 1c) to the addition of basal lateral glands, (Fig. 1d) to a central apical gland replacing the long central gland (Fig. 1e). Although new and expanded scales in 40-cm tall seedlings are more than twice as large as 20 cm seedlings, they maintain the configuration of an apical central and two basal and lateral glands (Fig. 1h, i), indicating that the changes in gland organization is complete. Fully grown basal scales and needles turn orange to dark-brown as they age (Fig. 1f, g).

Secondary, tertiary and quaternary shoots

The leaves at the base of a 2° shoot show a gradual transition from a needle shape to a scale shape similar to the transition of leaves along the primary shoot, with the one major difference; that the transition results in a bilaterally symmetric shoot (Fig. 2a, with magnification of base in Fig. 2b). In lateral scales, an increasingly greater portion of leaves is fused to the stem coupled with a gradual decrease in blade length (L1–L3 in Fig. 2b). Central leaves (C1–C3 in Fig. 2b) undergo a similar transition in shape, but most of the leaf surface remains fused to the stem, giving rise to a diamond or scale shape, as shown in C3 (Fig. 2b). The transitions in leaf shape along the axes of secondary shoots are companioned by changes in resin storage organs. In Fig. 2b, a central long duct is visible in the first central scale (C1) along with a lateral shorter structure. In subsequent scales, the central resin structure is gradually shorter, appearing as a spindle-shaped gland in the C3 scale (Fig. 2b). Glands are also visible in lateral scales (insets in Fig. 2b).

Scales of tertiary and quaternary shoots show the typical morphology of mature foliage, with lateral scales wrapping around the base of central scales, with no discernible internodes. A median apical resin gland can be seen in the central scales. The two sides of the foliage differ in that the adaxial side (Fig. 2c) is darker green than the abaxial side (Fig. 2d).

Fig. 3 Clearings revealing resin duct to resin gland transition. **a** *T. plicata* needle with a single resin duct that is runs through both free blade and stem-bound portion. **b** Shortened needle with a resin duct that ends before the base of the needle. **c** Further shortened needle with an elongated resin gland. **d** Typical scale with a predominant medial resin gland. **e** 3° shoot, (**f**, **g**) 4° shoot. *Arrows* point at resin ducts and glands. *Bars* 1 mm

Phase changes in the anatomy of resin storage structures

Partial clearings of leaves collected along the axis of the primary shoot show not only the transition from needles to scales, but also the parallel internal transition from resin ducts to resin glands. In a young seedling, a basal needle has a medial–abaxial duct along the entire length of the needle (Fig. 3a). Figure 3b shows a leaf further up the stem, with the shape of a needle, and a duct that tapers to an end before the base of the needle. The subsequent scale leaves contains a gradually shorter spindle-shaped gland (Fig. 3c, d). In ~25 cm tall seedlings, with dead basal needles that do not clear well, the same transition is nevertheless visible in live leaves along the primary shoot axis. In addition, lateral basal glands are apparent (Supplementary Figure 2).

The scales of 3° and 4° shoots have resin glands rather than ducts. Partial experimental clearings show that the numbers of glands vary with size of scales. Scales of the 4° shoot in Fig. 3f have the basic set of glands with a central, apical gland on both the adaxial and the abaxial side, and one gland in each of the lateral scales. In addition to this basic set of glands, the larger scales of 3° shoots also have additional glands in both central and lateral scales (Fig. 3e). Secondary shoots were too dense for clearings, and were approached by sectioning.

Cross-sections confirmed and extended the results obtained by clearings. In cross-sections of needles from young seedlings (5–10 cm tall), a single longitudinal medial resin duct is clearly visible just below the epidermis at the abaxial side both in the free blade (Fig. 4a, b). The basal portion of the needle that is fused to the stem also has one or two lateral ducts in addition to the central duct

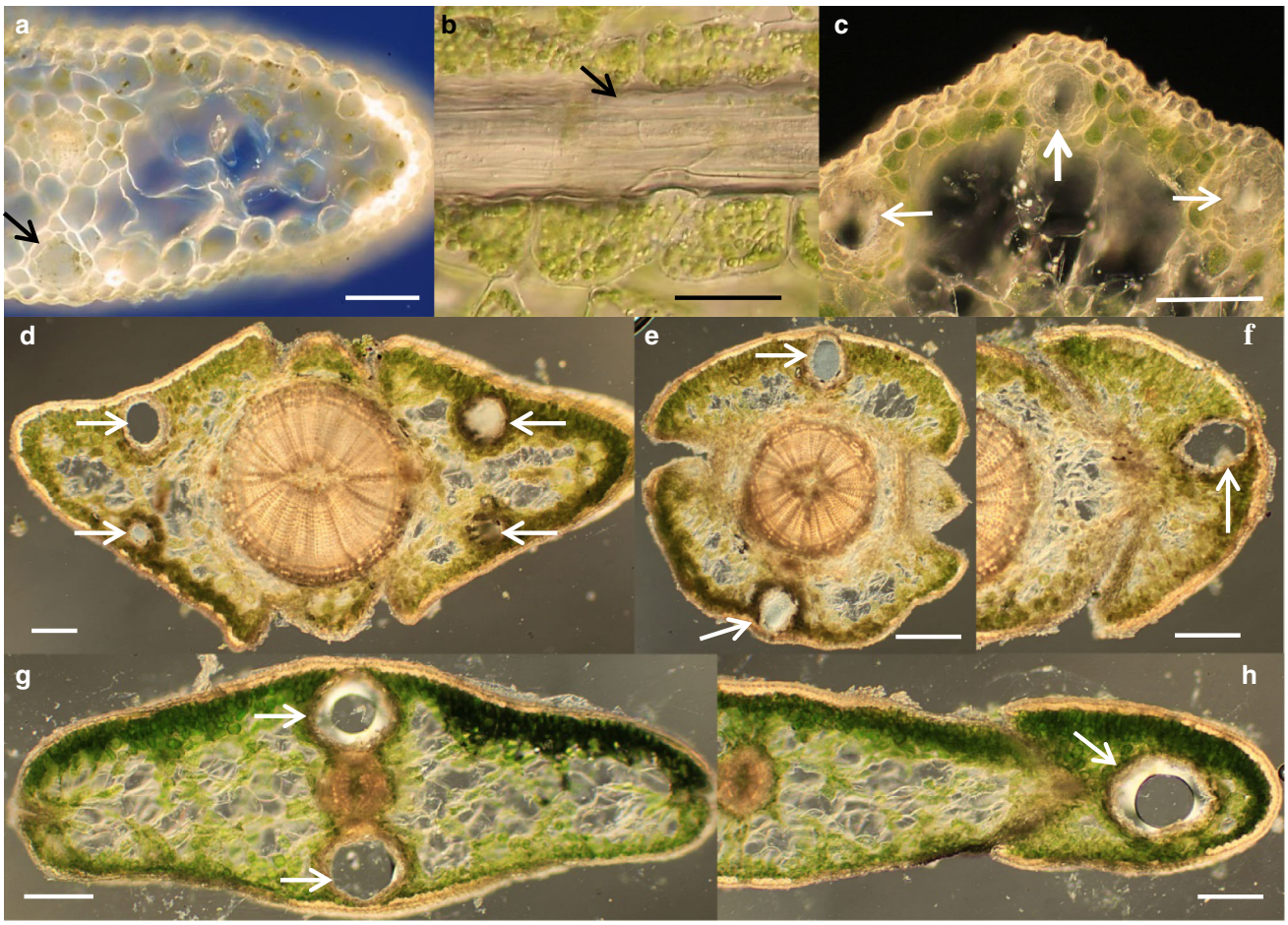

Fig. 4 Sections showing the positions of resin glands and resin ducts. **a** Cross section through a cleared *T. plicata* needle showing a single resin duct below the vascular bundle at the early phase. **b** Longitudinal-section though a fresh needle showing the continuous resin duct. **c** Cross-section through the primary shoot showing resin ducts in the portion of a needle that is fused to the stem, with *thick arrow* pointing at central duct, and thin arrows pointing at lateral ducts. Cross-sections of a secondary shoot at the level of the basal glands in lateral scales (**d**), apical glands of central scales (**e**), and the apical gland of a lateral scale (**f**). Cross-sections through a quaternary shoot at the level of apical central glands (**g**) and a lateral scale apical gland (**h**). *Arrows* point at gland epithelium of resin ducts and glands. *Size bars* 0.1 mm in **a**, **b**; 0.5 mm in **c**; 0.2 mm in **d**–**h**

(Fig. 4c). Figure 4d–f shows cross-sections of secondary shoot scale complexes, cut through the region with basal glands in the lateral scales (4d), a cut through the apical glands of the central scales (4e), and through the apical gland of a lateral scale (4f), revealing the bilateral symmetry of anatomy, including gland positions. The flat 3° and 4° shoots have a similar gland organization with medial glands in both abaxial and adaxial central scales (Fig. 4g) and apical glands in lateral scales (Fig. 4h). With the exception of the apical gland of lateral scales on 3° and 4° shoots (Fig. 4h), glands are adjacent to the hypo- and epidermis.

Anatomical barriers to the release of resin volatiles

To determine whether there is anatomical support for release of resin stored in ducts and glands into the atmosphere, we studied (1) if ducts and glands end at, or close to, the apices of needles and scales, (2) if there are anatomical indications of facilitated diffusion between resin structures and the atmosphere, and (3) if diffusion barriers develop around resin storage structures.

Duct and gland position relative to leaf apices

We used black autostaining of ducts and glands (see materials and methods) to visualize the position of the duct and gland cells relative to the apex of needles. In Fig. 5a–c, white arrows point at the apical-most black cells, with a mean distance of 0.60 mm ± 0.15 ($n = 15$) away from the tip. In transition-stage needles, the duct apex is farther away from the needle apex (Fig. 5d). Also, in leaves where the morphological transformation into scales appears complete but the central gland is still in a transitory stage, the gland apex is at a considerable distance from the leaf apex (Fig. 5e). In scales of lower-order branches, the glands are never close to the apices (not shown). In needles, hypodermal fiber cells run parallel to, and in close association with, duct cells (Fig. 5a–c). These fibers extend all the way to the apex of needles. Fibers are also found

Fig. 5 Position of resin ducts and resin glands relative to leaf apexes. **a–c** *T. plicata* needles with dark-staining duct epithelial cells (*arrows*) ending close to the apex. Tip of early (**d**) and late (**e**) needle-scale transition leaves with ends of glands (*white arrows*) and ends of xylem (*black arrows*). The photograph in (**d**) also shows a basipetal decreasing gradient of transfusion tracheids (*arrowheads*) away from the tip. **f** Dark-field of scale in (**e**), showing fibers mainly at and near the tip in the dissected abaxial side of the scale. *Size bars* 0.1 mm in **a–c**; 0.25 mm in **e**, **f**

sub-epidermal in needle-scale transition leaves and scales, and gland and fiber cells together can easily be interpreted as glands extending all the way to the apex in bright-field optics. The cell types can be separated, though, by visualizing the black staining gland cells in bright-field optics, and the dense fibers in either DIC or dark-field optics (compare Fig. 5e, f).

Duct and gland position relative to hypodermis and leaf surface

Thuja plicata foliage has a layer of dense fibers under the epidermis, typical of conifer needles, and known as the hypodermis (Figs. 6, 7). We used partially cleared samples to assess the coverage of hypodermis relative to resin ducts

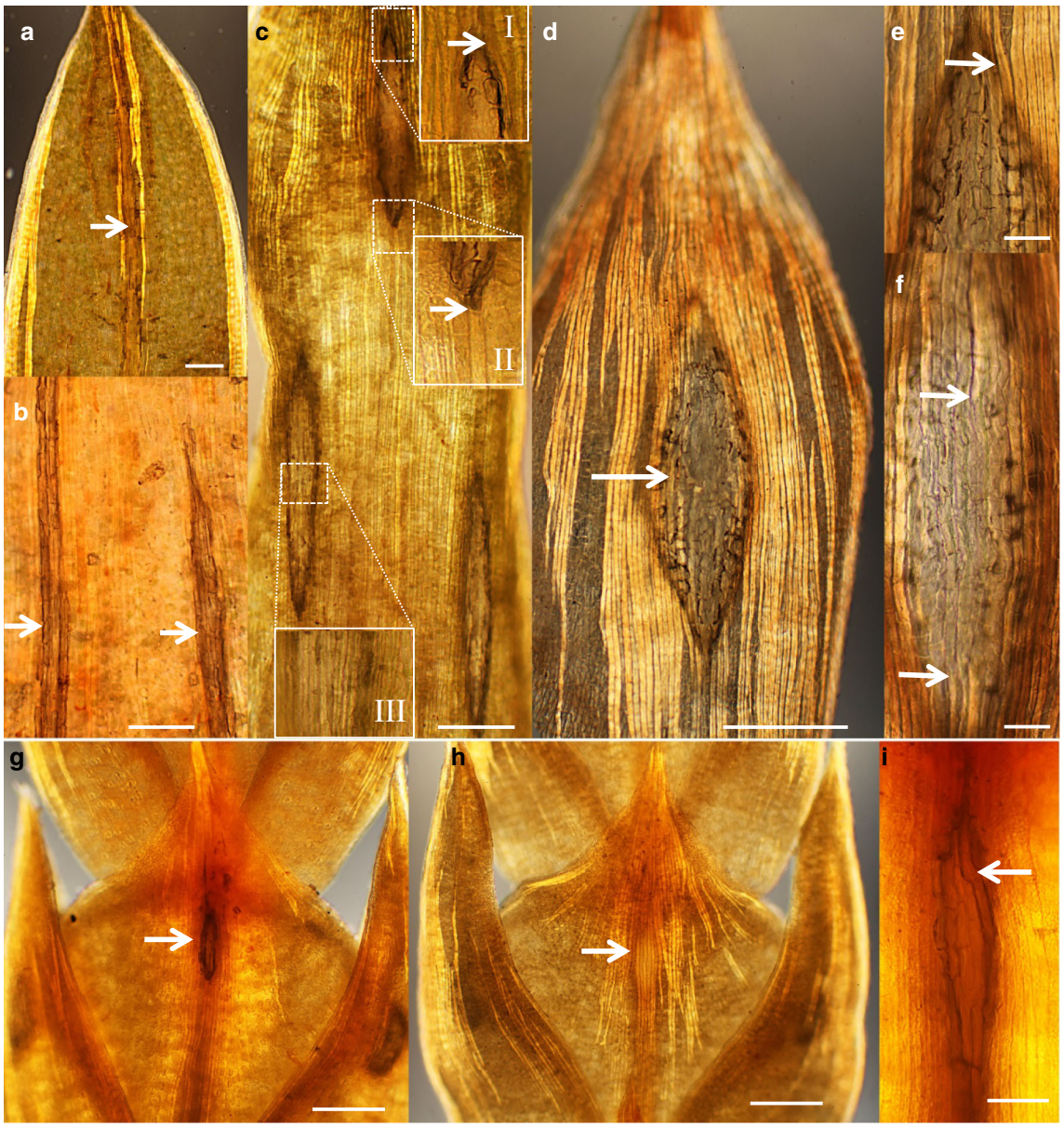

Fig. 6 Fiber coverage relative to resin ducts and resin glands. **a** *T. plicata* needle apex with dark-staining duct epithelial cells in the center (*arrow*), flanked by fibers. **b** Surface of the stem-bound portion of a needle showing the central duct (*left arrow*) and one of the two basal lateral ducts (*right arrow*), both covered by fibers. Primary stem of early (**c**) and late (**d**) needle-scale transition leaves. *Insets* in (**c**) indicate magnified areas of the apical end of the central gland with bending fiber (*arrow* in *I*), the basal end gland with fiber ending at gland (*arrow* in *II*), and the basal lateral gland showing striations indicating fiber coverage (*III*). The *arrow* in (**d**) points at gap in fiber layer above central apical gland, outlined by underlying dark gland epithelial cells. Magnifications of fiber coverage of the central apical gland of 1° apical scales showing bending fiber around gland (*arrow* in **e**), and fiber differentiation ending at gland (*arrows* in **f**). Quaternary shoot scales showing the apical gland of a central scale that is not covered by fibers (*arrow* in **g**) and covered by fibers (*arrow* in **h**). **i** Enlarged portion of a 4° shoot central gland with arrow pointing at bending fiber. *Size bars* 0.25 mm in **a**–**c**, **g**, **h**; 0.5 mm in **d**; 0.1 mm in **e**, **f**, **i**

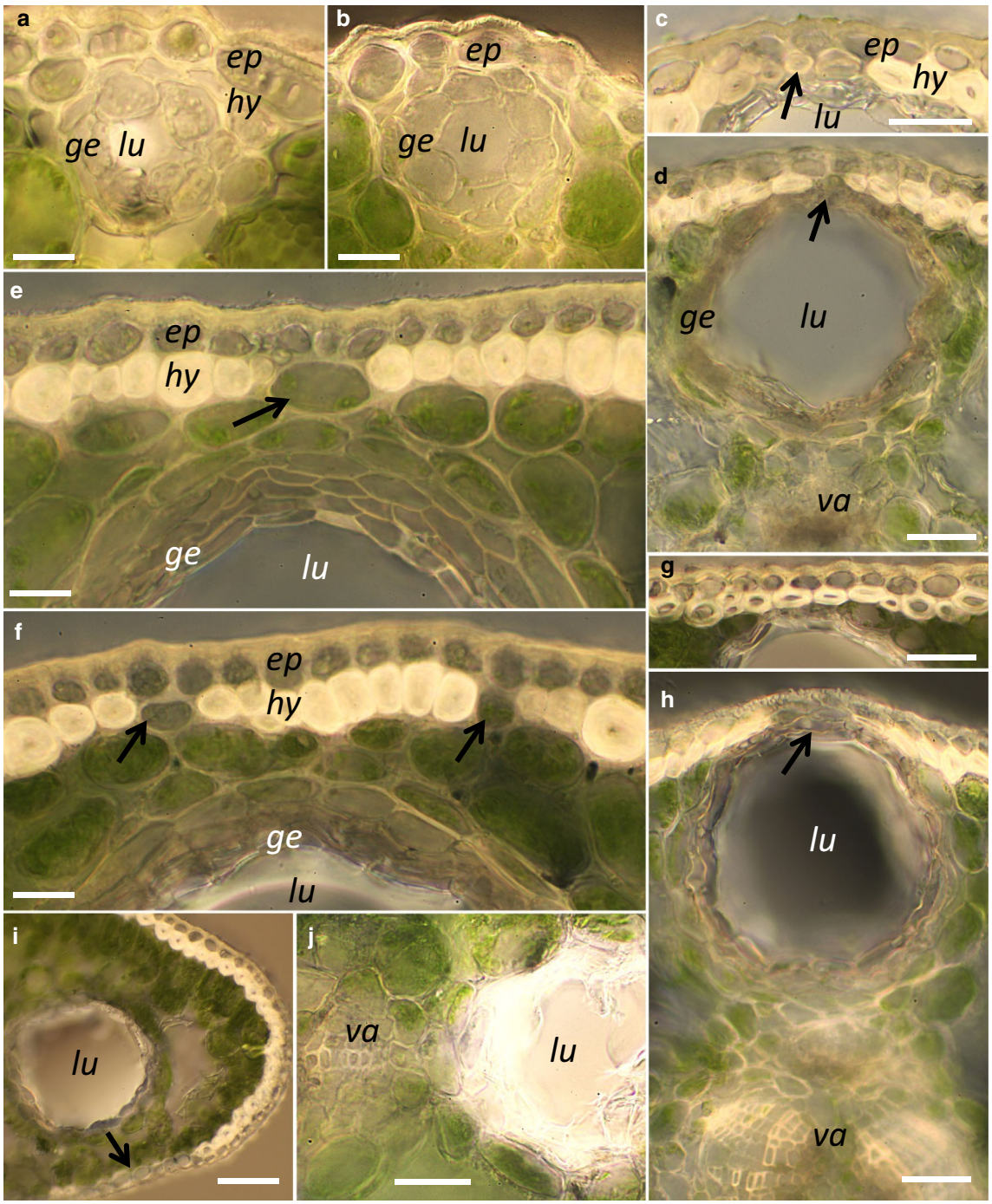

Fig. 7 Anatomy of resin ducts and resin glands relative to epidermis. *T. plicata* needle resin duct in region fused to stem (**a**) and in free blade (**b**). **c**, **d** Central apical gland of elongated primary stem scales. Central gland of central scales in secondary shoots (**e**, **f**) and in tertiary shoots (**g**, **h**). **i**, **j** Basal gland in tertiary shoot branch lateral scales. *Ep* epidermis, *hy* hypodermis, *ge* gland epithelium, *me* mesophyll, *lu* lumen of resin duct or gland, *va* vascular tissues. *Arrows* point at gaps in continuity of hypodermal fibers. *Size bar* 25 μm in **a**, **b**, **e**, **f**; 50 μm in **c**, **d**, **g**, **h**, **j**; 100 μm in **i**

and glands. In needles of the primary stem, the free blade has hypodermal fibers along the margin and at the tip, and some or no fibers flanking, but not covering, the abaxial central resin duct (Fig. 6a). The stem-bound portion of needles is almost completely covered with hypodermal fibers (Fig. 6b). In needle-to-scale-transition leaves, hypodermal fibers cover most of the abaxial surface, including basal lateral glands (Fig. 6c). The central apical gland, however, is typically not covered with fibers (Fig. 6c), and show hypodermal fibers that appear to bend around (insert

I) or stop short of (insert II) the gland area. This gap in the fiber layer above the central apical gland is even more pronounced in scales close to the apex of seedlings (Fig. 6d), again with fibers bending around (Fig. 6e), or fibers either ending at the gland area or exhibiting reduced cell-wall thickenings in the gland area (Fig. 6f). In clearings of scales of 3° and 4° shoots, the central apical resin gland appears either not covered (Fig. 6g) or covered (Fig. 6h). Fibers appear to bend around the site of glands (Fig. 6i). Whether or not a gland of scales in 3° and 4° shoots is covered with fibers varies even within individual shoots (Supplemental Figure 3).

High-magnification cross-section images show that ducts and glands are typically adjacent to the hypo- and epidermal layers. In most sections, there are gaps in the fiber layer at sites of ducts and glands, although they appear smaller than those seen in Fig. 6, possibly due to the absence of clearing. In primary stem needles, both in the stem-fused portion (Fig. 7a) and the free blade (Fig. 7b) the duct epithelium of the resin duct is adjacent to the epidermis. In primary stem scales, the central abaxial gland is separated from the epidermis by a hypodermis. However, fibers are either poorly differentiated (Fig. 7c) or single hypodermal cells are missing (arrow in Fig. 7d). In secondary shoots, the central scales also have gaps or poorly differentiated fibers in the layer of dense hypodermal fibers (Fig. 7e, f). Similarly, in tertiary or quaternary shoots, the central scales typically have a gap in the fiber layer between epidermis and gland (Fig. 7h), with some exceptions (Fig. 7g). Glands in lateral scales are not directly adjacent to epidermis, but are nevertheless companioned by poorly differentiated hypodermal fibers (Fig. 7i).

Position of ducts and glands relative to vascular tissues

In needles, the median–abaxial duct runs parallel, and within a few-cell-distance, to the midvein (Fig. 4a). In the stem-bound portion of needles, the distance can be larger as mesophyll cells expand (Fig. 4c). In needle-scale transition leaves of primary stems, the midvein runs closer to the apex than the duct and is extended by transfusion tracheids close to the leaf tip (Fig. 5d, e; also shown in Aloni et al. 2013). In central scales of 1°, 2° and 3° shoots, the central glands are within a few-cell-distances from the central vascular cylinder (Fig. 7d, h), and they are connected by transfusion tracheids. Also glands of later scales are in close proximity to vascular strands (Fig. 7j).

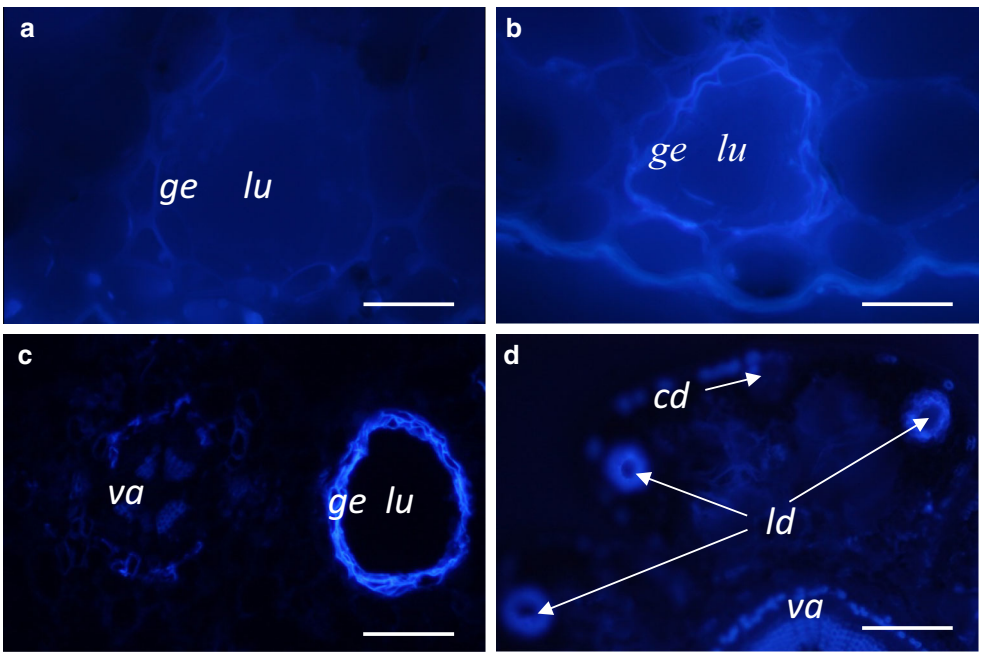

Fig. 8 UV epifluorescence from resin duct and gland epithelium cells. **a** Resin duct from a newly formed *T. plicata* needle showing no cell wall fluorescence. **b** Resin duct from an older needle showing autofluorescence compared to the cell of the surrounding parenchyma and epidermal tissue. **c** Scale showing a resin gland with strong cell wall autofluorescence compared to that of the vascular tissue (V). **d** Stem section from the basal stem-bound portion of needles, showing strong autofluorescence in lateral ducts (*ld*), but not in central duct (*cd*). *Lu* lumen of duct or gland, *ge* duct or gland epithelium, *va* vascular bundle. *Size bars* 100 μm in **a**, **b**; 300 μm in **c**; 800 μm in **d**

Cell wall deposits

We studied the cell walls surrounding resin storage structures in *T. plicata* to determine whether ducts and glands differ with respect to potential diffusion barriers such as suberin or lignin. For these studies, we used autofluorescence as a useful indicator of these polyphenolics. Resin ducts and resin glands in sections of needles and scales differ significantly in autofluorescence. Fluorescence intensity also differs based on the maturity of the resin storage structures. The cell walls of epithelial cells surrounding the resin ducts in newly formed needles show little to no autofluorescence (Fig. 8a). As the needle matures, fluorescence gradually increases in the resin duct cell walls of the oldest needles (Fig. 8b). The same trend of autofluorescence increasing with age was apparent with resin glands. In newly formed scales, resin glands do not show autofluorescence, but as the leaf ages, gland-cell-wall autofluorescence rapidly increases (Fig. 8c). In needle-scale transition leaves, lateral glands show strong autofluorescence whereas central ducts do not (Fig. 8d).

Monoterpene profiles of needles and scales

Based on the three *T. plicata* genotypes we analyzed, there are quantitative and qualitative differences in the monoterpenoid profiles of needles and scales. The total monoterpene content is at least four times higher in scales than in needles (Fig. 9b). In scales, α-thujone is by far the most abundant monoterpene and occurs at levels 20-fold higher than in needles (Fig. 9c). β-Thujone is also much more abundant in scales than in needles but the overall amount is lower (Fig. 9e). Sabinene, the suspected biosynthetic precursor to thujone, was significantly up-regulated in the scales of two genotypes (Fig. 9d). The amounts of several other monoterpenes, such as myrcene, (+)-α-pinene, (+)-limonene, and α-thujene, are several-fold higher in scales than in needles (Fig. 9f, h–j). In contrast, the amount of (+)-β-pinene appeared higher in needles than in scales, but this difference was significant for only one of the three genotypes studied. Following (+)-sabinene, (−)-α-pinene is the second most abundant monoterpene in needles (Supplementary Figure 4a) but is not detectable in scales (Fig. 9g). (+)-Sabinene is the second most abundant monoterpene in scales, greatly surpassed by its suspected product, α-thujone (Supplemental Figure 4b).

Discussion

Our study was motivated by the quest to understand the anatomical and ontogenetic bases of monoterpenoid production to determine underlying genetic differences in foliar monoterpenoid content between provenances of *T. plicata*. We focused on internal ducts and glands because in many species they are well known to store monoterpenoids, and because foliage extracts of a natural *T. plicata* variant that lacks foliar glands also lacks monoterpenoids (Foster et al. 2013). Although not widely recognized as such, *T. plicata* leaves undergo phase changes including a switch from a needle shape typical of many conifers, to small, tightly-packed scales. We show that leaf-phase changes are accompanied by equally significant changes in terpenoid storage structure shape, wall characteristics, as well as changes in monoterpenoid levels and composition. Here, we will first summarize our findings and thereafter discuss them in the light of related literature.

Briefly, cotyledons lack resin storage structures, needles have an abaxial–medial resin duct, and needle-scale transition-stage leaves have basal lateral glands in addition to a shortening medial resin duct. Central and lateral scales have a short medial gland close to the apex, and larger scales have a variable number of lateral resin glands. We found evidence for (1) a gradual ontogenetic transition of resin structures in the needle-to-scale transition zone along the primary shoot axis, supporting Suzuki's (1979) concept and (2) a steeper transition at the base of secondary shoots.

We also found that needles and scales differ considerably in the content and composition of monoterpenoids. Scales hold four to eight times more monoterpenoids than needles. Needles also contain almost exclusively pure monoterpene hydrocarbons and lack oxygenated monoterpenoids. Compared to needles, scales incorporate higher levels of five out of six detected monoterpenes. In scales, the production of the monoterpene hydrocarbon (−)-α-pinene was turned off, and the production of (+)-α-pinene and of oxygenated α- and β-thujone was turned on. As juvenile *T. plicata* seedlings share features such as needles, ducts and a propensity for monoterpene hydrocarbons with distantly related conifers (e.g., Pinaceae), it is possible that these are ontogenetic remnants from a common phylogenetic origin. Similar transitions from hydrocarbon to oxygenated monoterpenes in juvenile to adult foliage occur in other members of the cypress family such as *Sequidoiadendron giganteum* and *Juniperus scopulorum* (Adams and Hagerman 1977; Levinson et al. 1971) but are absent in *Juniperus horizontalis* where juvenile and mature foliage have similar leaf resin compositions (Adams et al. 1980). Several arguments can be made why a switch from pure hydrocarbon monoterpenes to oxygenated monoterpenes could be beneficial. First, oxygenated monoterpenes are generally more biotoxic than hydrocarbon monoterpenes (Vaughn and Spenser 1993), providing seedlings that develop mature scale foliage with improved defenses. This concept is supported by observations that the oxygenated

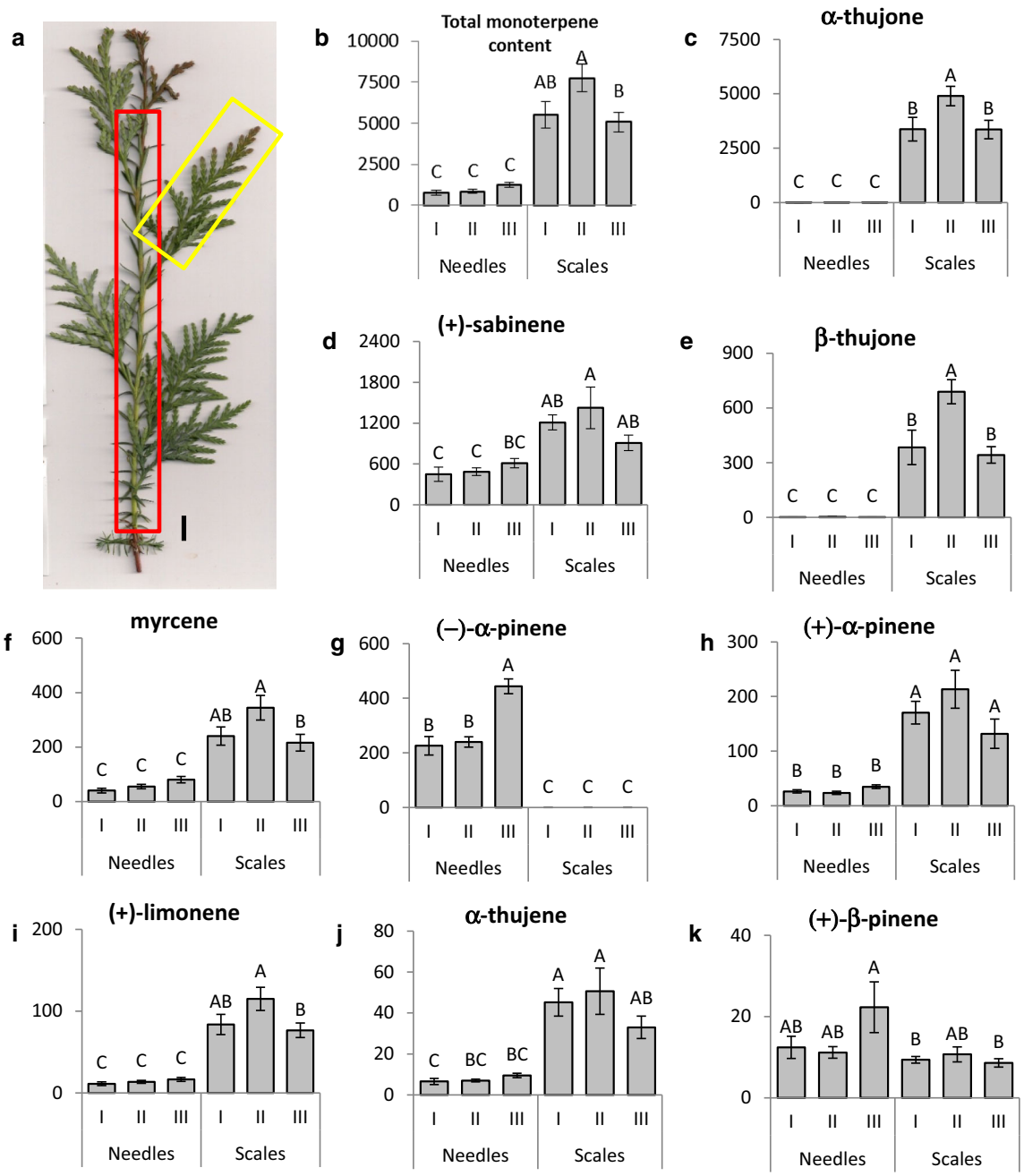

Fig. 9 Monoterpenoid content of needles and scales of *T. plicata* seedlings. Primary shoot with needles (*red box*) and secondary shoot with scale leaves (*yellow box*). **b–k** Mean abundance (±SE) of total and individual monoterpenoids in needles and scales (μg/g fresh-weight foliage). Roman numerals indicate pooled data from clones: *I* 45052, *II* 45010 and *III* 63110. In each *subpanel*, *bars* with *different letter superscripts* are significantly different ($P < 0.05$; Tukey's HSD test). *Scale bar* in *subpanel* (**a**): 1 cm

monoterpenes α- and β-thujone are highly effective feeding deterrents against three species of deer, whereas the hydrocarbon monoterpenes α-pinene, sabinene, limonene and myrcene are only marginally deterrent (Vourc'h et al. 2002b). Secondly, oxygenated monoterpenoids dissolve in water much more readily than hydrocarbon monoterpenes (Weidenhamer et al. 1993; Fichan et al. 1999). Therefore, the oxygenated thujones are more likely than hydrocarbon monoterpenes to diffuse within tissues as well as out of plants, thus potentially contributing to both internal systemic defenses and improved emission into the surrounding air. A tradeoff to both enhanced biotoxicity and water solubility is increased auto-toxicity (LaPasha and Wheeler 1990), which could explain our observation of stronger polyphenol diffusion barriers around glands in scales relative to needles.

As *T. plicata* seedlings release substantial amounts of volatile terpenes into the atmosphere (Kimball et al. 2005; Burney et al. 2012), we looked for potential adaptations that could facilitate terpene release into the environment. We found no anatomical evidence that ducts or glands open directly to the air at the apexes of needles or scales. This is perhaps not surprising as resin-producing epithelia would then easily be subject to rapid loss of volatile monoterpenoids as well as water. On the other hand, we found several anatomical features that are in line with paths of reduced resistance to diffusion of terpenoids out of the foliage. First, ducts are directly adjacent to the epidermis, and glands are separated from the epidermis by only a single layer of fibers and 0–2 layers of mesophyll cells. Second, there are typically either gaps in the fiber layer or reduced wall densities of fiber cells between ducts and glands and the epidermis. Third, glands and ducts are in close proximity to spongy mesophyll and vascular cells including transfusion tracheids. Thus, monoterpenoids need only diffuse a short distance from glands before exiting directly via leaf air-spaces and stomata or indirectly via the xylem, mesophyll, leaf air-spaces and stomata. Fourth, ducts and young glands show no or little UV autofluorescence in the surrounding cell walls, indicative of lignin or suberin depositions and hence reduced resistance to diffusion relative to older structures. The close proximity of ducts and glands to the waxy cuticle opens up the possibility that waxes are locally dissolved by released terpenoids, facilitating diffusion out of tissues. That terpenes have the capacity to dissolve waxes is illustrated by the use of terpenes as a substitute for the highly toxic xylene in paraffin infiltration and removal procedures in histology laboratories (Wynnchuk 1994).

We also saw variation in the number of glands in scales, with larger scales having more glands than smaller scales, and also variation in the fiber coverage of glands, begging the question of what might regulate the variation in these traits. The rate of resin duct formation in the xylem of *P. halepensis* is affected by pressure, wind, wounding and growth substances (Fahn and Zamski 1970). The application of the ethylene-releasing agent ethrel (2-chloroethylphosphonic acid) to *P. halepensis* seedlings promotes the production of longitudinal resin ducts (Yamamoto and Kozlowski 1987). Methyl jasmonate, which activates defense-related genes, seems to be the primary signal which induces traumatic resin-duct formation in conifers (Hudgins et al. 2003; Hudgins and Franceschi 2004; Schmidt et al. 2011), and this jasmonate-induced defense response is mediated by ethylene (Hudgins and Franceschi 2004).

On the other hand, ethylene inhibits fiber differentiation (Aloni et al. 1998; Aloni 2013a). The fibers are induced by streams of combined high-gibberellin with low-auxin levels (Aloni 2013b, 2015). The longitudinal patterns of sub-epidermal fiber bundles, from the scale's tip to its base, usually avoiding the glands (Fig. 6, Supplemental Figure 3), likely indicate a local inhibition of fiber differentiation at the gland sites. Therefore, we hypothesize that at the site of a differentiating gland, an elevated local ethylene concentration, which promotes resin-duct formation (Yamamoto and Kozlowski 1987), is the inhibiting signal that prevents sub-epidermal fiber differentiation above the differentiating gland by antagonizing the fiber-inducing effect of gibberellin. The resulting pattern of fiber differentiation away from the glands, which forms gaps in the sub-epidermal fiber layer, facilitates the diffusion of monoterpenoids from the leaf.

A recent study showed that the monoterpenoid content of *T. plicata* seedlings varies over the year, peaking in the winter, and also depended upon the availability of nitrogen and phosphorous (Burney et al. 2012). Here we show that primary shoot needles and secondary shoot scales differ considerably both quantitatively and qualitatively with respect to monoterpenoids. Together, these studies provide a framework for comparative phenotyping of monoterpenoid profile and content.

Conclusions

Leaf-phase changes in young *T. plicata* plants are companied by internal changes in resin storage structures as well as the composition and level of stored monoterpenoids. Total monoterpene content and composition differ markedly between needles and scales. Monoterpene content is multifold higher in scales than in needles, and the abundance of (−)-α-pinene in needles shifts to an abundance of thujones in scales. Our results also have bearing on *T. plicata* breeding programs aimed at reducing deer browsing. When breeding for high thujone content as the major deterrent against ungulate herbivory, needles should be excluded for monoterpenoid quantifications and plantlets dominated by thujone-containing scale foliage should be considered for reforestation. We also reveal anatomical features that may affect release of monoterpenoids and thus the food choice of herbivores. Examples are the close proximity of glands to the epidermis and gaps in the hypodermis layer above glands that may facilitate release, and polyphenolic linings that develop around aging glands that may limit release. These anatomical features provide new markers for phenotype–genotype association studies underway in this species.

Author contribution statement A.J.F., R.A. and J.M. carried out the anatomical analysis. A.J.F., M.F., G.G. and R.G. carried out the analysis of monoterpenoid content. J.M. and A.J.F. wrote the manuscript. All authors provided feedback on the manuscript.

Acknowledgments We thank Dr. John Russell for introducing us to the "problem" of resin production in *T. plicata* foliage and anonymous reviewers for constructive comments on the manuscript.

Compliance with ethical standards

Conflict of interest The authors declare that they have no conflict of interest.

References

Adams RP, von Rudloff E, Hogge L, Zanoni TA (1980) The volatile terpenoids of *Juniperus monticola f. monticola*, *f. compacta*, and *f. orizabensis*. J Nat Prod 43:4–17

Adams RP, Hagerman A (1977) Diurnal Variation in the Volatile Terpenoids of Juniperus scopulorum (Cupressaceae). Am J Bot 64:278–285

Aloni R (2013a) The role of hormones in controlling vascular differentiation. In: Fromm J (ed) Cellular aspects of wood formation. Springer, Berlin, pp 99–139

Aloni R (2013b) Role of hormones in controlling vascular differentiation and the mechanism of lateral root initiation. Planta 238:819–830

Aloni R (2015) Ecological implications of vascular differentiation and plant evolution. Trees 29:1–16

Aloni R, Wolf A, Feigenbaum P, Avni A, Klee HJ (1998) The *Never ripe* mutant provides evidence that tumor-induced ethylene controls the morphogenesis of *Agrobacterium tumefaciens*-induced crown galls on tomato stems. Plant Physiol 117:841–849

Aloni R, Foster A, Mattsson J (2013) Transfusion tracheids in the conifer leaves of *Thuja plicata* (Cupressaceae) are derived from parenchyma and their differentiation is induced by auxin. Am J Bot 100:1949–1956

Biggs AR (1985) Detection of impervious tissue in tree bark with selective histochemistry and fluorescence microscopy. Stain Technol 60:299–304

Bohlmann J, Steele J, Croteau R (1998) Monoterpene synthases from grand fir (*Abies grandis*). cDNA isolation, characterization, and functional expression of myrcene synthase, (−)-(4S)-limonene synthase, and (−)-(1S, 5S)-pinene synthase. J Biol Chem 272:21784–21792

Burney OT, Davis AS, Jacobs DF (2012) Phenology of foliar and volatile terpenoid production for *Thuja plicata* families under differential nutrient availability. Environ Exp Bot 77:44–52

Chu FH, Kuo PM, Chen YR, Wang SY (2009) Cloning and characterization of α-pinene synthase from *Chamaecyparis formosensis* Matsum. Holzforschung 63:69–74

Fahn A, Zamski E (1970) The influence of pressure, wind, wounding and growth substances on the rate of resin duct formation in *Pinus halepensis* wood. Isr J Bot 19:429–446

Fichan I, Larocche C, Gros JB (1999) Water solubility, vapor pressure, and activity coefficients of terpenes and terpenoids. J Chem Eng Data 44:56–62

Foster AJ, Hall DE, Mortimer L, Abercromby S, Gries R, Gries G, Bohlmann J, Russell J, Mattsson J (2013) Identification of genes in *Thuja plicata* foliar terpenoid defenses. Plant Physiol 161:1993–2004

Gesell A, Blaukopf M, Madilao L, Yuen MM, Withers SG, Mattsson J, Russell JH, Bohlmann J (2015) The gymnosperm cytochrome P450 CYP750B1 catalyzes stereospecific monoterpene hydroxylation of (+)-sabinene in thujone biosynthesis in western redcedar. Plant Physiol 168:94–106

Goebel K (1913) Organographie der Pflanzen. 1. Teil: Allgemeine Organographie. Jena, Gustav Fischer

Gonzalez JS (2004) Growth properties and uses of western red cedar. Forintek Canada Corp. Special Publication, No. SP-37R

Hudgins JW, Franceschi VR (2004) Methyl jasmonate-induced ethylene production is responsible for phloem defense responses and reprogramming of stem cambial zone for traumatic resin duct formation. Plant Physiol 135:2134–2149

Hudgins JW, Christiansen E, Franceschi VR (2003) Methyl jasmonate induces changes mimicking anatomical defenses in diverse members of the Pinaceae. Tree Physiol 23:361–371

Kaplan DR (1980) Heteroblastic leaf development in Acacia—morphological and morphogenetic implications. Cellule 73:135–203

Kimball BA, Russell JH, Griffin DL, Johnston JJ (2005) Response factor considerations for the quantitative analysis of western redcedar (*Thuja plicata*) foliar monoterpenes. J Chromatogr Sci 43:253–258

Langenheim JH (1969) Amber: a botanical inquiry. Science 163:1157–1169

Langenheim JH (1990) Plant resins. Am Sci 78:16–24

Langenheim JH (1994) Higher plant terpenoids: a phytocentric overview of their ecological roles. J Chem Ecol 20:1223–1280

Lapasha CA, Wheeler EA (1990) Longitudinal canal lengths and interconnections between longitudinal and radial canals. IAWA Bull 11:227–238

Levinson AS, Lemone G, Smart EC (1971) Volatile oil from foliage of *Sequiadendron giganteun*: change in composition during growth. Phytochem 10:1087–1094

Lin J, Jack ME, Ceulemans R (2001) Stomatal density and needle anatomy of Scots pine (*Pinus sylvestris*) are affected by elevated CO_2. New Phytol 150:665–674

Martin J, Baltzinger C (2002) Interaction among deer browsing, hunting and tree regeneration. Can J For Res 32:1254–1264

Martin J, Daufresne T (1999) Introduced species and their impacts on the forest ecosystem of Haida Gwaii. In: Wiggins G (ed) Proceedings of the cedar symposium: growing western redcedar and yellow-cypress on the Queen Charlotte Islands/Haida Gwaii. British Columbia South Moresby Forest Replacement Account, BC Ministry of Forests and Ranges, Victoria, pp 69–83

Rosner S, Hannrup B (2004) Resin canal traits relevant for constitutive resistance of Norway spruce against bark beetles: environmental and genetic variability. For Ecol Manag 200:77–87

Russell JH (2008) Deployment of deer resistant western redcedar (*Thuja plicata*). USDA Forest Service Proceedings. RMRS-P57:149–153

Schmidt A, Nagel R, Krekling T, Christiansen E, Gershenzon J, Krokene P (2011) Induction of isoprenyl diphosphate synthases, plant hormones and defense signalling genes correlates with traumatic resin duct formation in Norway spruce (*Picea abies*). Plant Mol Biol 77:577–590

Stroh N, Baltzinger C, Martin J (2008) Deer prevent western redcedar (*Thuja plicata*) regeneration in old-growth forests of Haida Gwaii: is there a potential for recovery? For Ecol Manag 255:3973–3979

Suzuki M (1979) The course of resin canals in the shoots of conifers II. Araucariaceae, Cupressaceae and Taxodiaceae. J Plant Res 92:253–274

Taiz L, Zeiger E (2010) The shoot apex and phase changes. Plant physiology, 5th edn. Sinauer Associates, Sunderland, pp 726–730

Unsicker SB, Kunert G, Gershenzon J (2009) Protective perfumes: the role of vegetative volatiles in plant defense against herbivores. Curr Opin Plant Biol 12:479–485

Vaughn SF, Spenser GF (1993) Volatile monoterpenes as potential parent structures for new herbicides. Weed Sci 41:114–119

Von Rudloff E, Lapp MS, Yeh FC (1988) Chemosystematic study of *Thuja plicata*: multivariate analysis of leaf oil terpene composition. Biochem Syst Ecol 16:119–125

Vourc'h G, Russell J, Martin J (2002a) Linking deer browsing and terpene production among genetic identities in *Chamaecyparis nootkatensis* and *Thuja plicata*. Heredity 93:370–376

Vourc'h G, Garine-Wichatitsky M, Labbé A, Rosolowski D, Martin J, Fritz H (2002b) Monoterpene effect on feeding choice by deer. J Chem Ecol 28:2411–2427

Vourc'h G, Vila B, Gillon D, Escarré J, Guibal F, Fritz H, Clausen TP, Martin J (2002c) Disentangling the causes of damage variation by deer browsing on long-lived tree saplings: a chemical and dendrochronological approach. Oikos 98:271–283

Weidenhamer JD, Macias FA, Fischer NH, Williamson GB (1993) Just how insoluble are monoterpenes? J Chem Ecol 19:1799–1807

Werker E, Fahn A (1969) Resin ducts of *Pinus halepensis* Mill.—their structure, development and pattern of arrangement. Bot J Lin Soc 62:379–411

White EE, Nilsson JE (1984) Genetic variation in resin canal frequency and relationship to terpene production in foliage of *Pinus contorta*. Silvae Genet 22:79–84

Wynnchuk A (1994) Evaluation of xylene substitute for paraffin tissue processing. J Histotechnol 17:143–149

Yamamoto F, Kozlowski TT (1987) Effect of ethrel on growth and stem anatomy of *Pinus halelensis* seedlings. IAWA Bull New Ser 8:11–19

Zotz G, Wilhelm K, Becker A (2011) Heteroblasty—a review. Bot Rev 77:109–144